



## A Practical and Single-Use ITO-Pet Based Immunosensing Platform for Detection of Tumor Necrosis Factor-Alpha Biomarker

### Tümör Nekrozis Faktörü-Alfa Biyobelirteç Tayini için Pratik ve Tek Kullanımlık ITO-PET Bazlı İmmunosensör Platformu

Burcu Özcan<sup>✉</sup>

Faculty of Engineering, Department of Bioengineering, Çanakkale Onsekiz Mart University, Çanakkale, Türkiye.

#### ABSTRACT

This investigation displays a novel, practical indium tin oxide- polyethylene terephthalate (ITO-PET) based electrochemical biosensor for the Tumor Necrosis Factor-alpha (TNF $\alpha$ ) biomarker determination. The ITO-PET electrode is a very advantageous preferred semiconductive electrode material. It has a lot of great features such as easy to prepare, cheapness, flexibility, stability. It also allows determining an analyte at very low concentrations and provides a great wide concentration range for analyte analysis. Electrochemical Impedance Spectroscopy (EIS) and Cyclic Voltammetry (CV) were used for the evaluation of biosensors, including the immobilization procedure, the investigation of the optimum conditions, and the characterization of biosensors. The immunosensor's electrode surface morphology during the immobilization process was observed using a Scanning Electron Microscope (SEM). In addition, Impedance measurement at a single frequency was used to characterize anti-TNF $\alpha$  and TNF $\alpha$  interactions (SFI). The clinical effectiveness of the developed biosensor was investigated by testing it with real human serum samples. Moreover, the fabricated immunosensor presents long shelf life, analysis of the antigen concentrations at picogram level (0.02 pg mL<sup>-1</sup> -2.56 pg mL<sup>-1</sup>), reproducibility, reusability and high sensitivity

#### Key Words

TNF $\alpha$ , immunosensor, ITO-PET electrode, electrochemical impedance spectroscopy.

#### ÖZ

Bu araştırma, Tümör Nekrozis Faktörü-alfa (TNF $\alpha$ ) biyobelirteç tayini için yeni, pratik bir indiyum kalay oksit-polietilen tereftalat (ITO-PET) bazlı elektrokimyasal biyosensörü göstermektedir. ITO-PET elektrodu çok avantajlı olarak tercih edilen bir yarı iletken elektrot malzemesidir. Hazırlanmasının kolay olması, ucuz olması, esnekliği, sağlamlığı gibi bir çok iyi özelliği vardır. Ayrıca çok düşük konsantrasyonlarda bir analitin belirlenmesine izin verir ve analit analizi için çok geniş bir konsantrasyon aralığı sağlar. İmmobilizasyon prosedürü, optimum koşulların araştırılması ve biyosensörlerin karakterizasyonu dahil olmak üzere biyosensörlerin değerlendirilmesi için Elektrokimyasal Empedans Spektroskopisi (EIS) ve Döngüsel Voltametri (CV) kullanıldı. İmmünosensörün immobilizasyon işlemi sırasında elektrot yüzey morfolojisi bir Taramalı Elektron Mikroskobu (SEM) kullanılarak gözlemlendi. Ayrıca, anti-TNF $\alpha$  ve TNF $\alpha$  etkileşimlerini karakterize etmek için tek bir frekansta empedans (SFI) ölçümü kullanıldı. Geliştirilen biyosensörün klinik etkinliği, gerçek insan serum numuneleri ile test edilerek araştırıldı. Ayrıca, tasarlanan immünosensör uzun raf ömrü, pikogram düzeyinde antijen konsantrasyonlarının analizi (0.02 pg mL<sup>-1</sup> -2.56 pg mL<sup>-1</sup>), tekrar üretilebilirlik, yeniden kullanılabilirlik ve yüksek hassasiyet sunar.

#### Anahtar Kelimeler

TNF $\alpha$ , immunosensör, ITO-PET elektrot, elektrokimyasal impedans spektroskopisi.

**Article History:** Received: Dec 7, 2022; Revised: Jan 17, 2023; Accepted: Jan 20, 2023; Available Online: Mar 7, 2023.

**DOI:** <https://doi.org/10.15671/hjbc.1215813>

**Correspondence to:** B.Özcan, Department of Bioengineering, Çanakkale Onsekiz Mart University, Çanakkale, Turkey.

**E-Mail:** burcuozcan@comu.edu.tr

## INTRODUCTION

One of the cytokines that sets off the acute phase reaction is tumour necrosis factor-alpha (TNF $\alpha$ ), a cell signalling protein implicated in systemic inflammation [2, 3]. TNF $\alpha$  is a member of the TNF superfamily [4], which consists of several transmembrane proteins with a homologous TNF domain [5]. The primary role of TNF $\alpha$  is the regulation of immune cells [6]. TNF, an endogenous pyrogen, can trigger a fever, apoptotic cell death [7], cachexia, and inflammation, suppress tumorigenesis and viral replication (virus replication) [8], and respond to sepsis through cells which produce Interleukin-1 and Interleukin-6 [9]. Disorder of TNF $\alpha$  secretion causes various diseases such as Alzheimer's disease, cancer [10], major depression, psoriasis and inflammatory bowel disease (IBD) [11]. TNF $\alpha$  is a candidate for the role of a biomarker in a variety of diseases, including rheumatoid arthritis, lung cancer, diabetes, HIV infection, neurodegenerative illnesses (Parkinson's, Alzheimer's, etc), heart failure, colon cancer, leukemia, stroke, and epithelial ovarian cancer [12-14].

Biosensors are advantageous and favored devices that are utilized to control target analyte materials in biological reactions and possess sensing capabilities [15]. Biosensors typically perform their functions as a result of a selective, rapid, and continuous reaction to a biologically or chemically active substance [16,17]. The advantages of biosensor-based devices include high sensitivity, rapid processing, measurements, and low cost [18]. Positive advances in electrochemical biosensors have been created in the areas of clinical diagnosis, environmental monitoring and food processing quality control [19]. Particularly, electrochemical biosensors for monitoring biomolecular interactions have enabled reagent-free, non-invasively, label-free, in-situ, on-site, online measurements of important parameters in a wide range of matrices or media. [20]. These functional characteristics are essential for the accurate diagnosis of many cancers and other diseases with significant clinical relevance [21]. Cancer has the highest mortality rate of any disease for which the effectiveness of current or future treatment options is a known factor in whether or not the patient survives. So, electrochemical biosensors have become more popular in the quest for ideal diagnostic techniques [22]. EIS is an experimental technique that measures impedance at the electrode-electrolyte interface very precisely as a frequency (time) dependent function. EIS is a powerful tool for studying electrochemical setups and procedures [23].

Recent years have seen the rise of advanced flexible and wearable electronics such as foldable mobiles, cheap photodetectors, flat panel displays and other disposable electronic devices. Since indium tin oxide (ITO, In<sub>2</sub>O<sub>3</sub>:Sn) thin films have high transmittance in the visible region and excellent electrical conductivity, they have found widespread application in biosensors [24], electronic, and optoelectronic devices. [25]. Rather than using heavy and easily broken glass, manufacturers of flexible electronics are increasingly interested in using lightweight and durable polyethylene terephthalate (PET) to deposit high-quality ITO thin films [26].

In the design of biosensors, silane chemistry is frequently utilized. Functional groups on the molecule of a silane coupling agent allow it to form bonds with both organic and inorganic substances [27]. This property is what makes silane coupling agents useful for increasing the mechanical strength of composite materials, enhancing adhesion, and modifying resins and surfaces [28]. During the formation of a monolayer, the carboxyethylsilanetriol (CEST) coupling agent interacts with hydroxylated ITO substrates. Due to their low interfacial tension, organofunctional silanes may be extremely reactive with various surfaces [29].

The novel contribution of the study was the simple performance of an impedimetric-based biosensor for TNF- $\alpha$  detection using a single-use, cheap and practical ITO-PET electrode. By combining the CEST silanization agent with the cost-efficient ITO-PET working electrode platform, a simple and stable immunosensor for TNF $\alpha$  detection was created in this work. The silanization process provided an excellent layer for the covalent binding of the antibody. In addition to providing a large surface area for immobilizing the anti-TNF $\alpha$ , the silanization solution also served as a stabilizing agent for the working electrode. TNF $\alpha$  antigen concentration was measured using EIS by reading the electrochemical signal produced after adding TNF $\alpha$  antigen to the anti-TNF $\alpha$  immobilized ITO-PET electrode. EIS and CV methods were used to analyze the immobilization procedures, determine the optimal parameters, and characterize the processes. The kinetics of anti-TNF $\alpha$  and TNF $\alpha$  interactions were studied using the Single Frequency Technique. Scanning electron microscopy (SEM) was used to observe the electrode surfaces throughout the various stages of modification to determine their morphology. The constructed immunosensor exhibited a high degree of sensitivity, excellent reproducibility, and a significant application potential in human serum.

## MATERIALS and METHODS

### Reagents, Devices and Electrochemical Procedures

The electrodes of the triple system, a platinum (Pt) counter electrode and a silver (Ag) and silver chloride (AgCl) reference electrode, were acquired from iBAS in Warwick, United Kingdom. The flexible ITO-PET electrodes were bought from Sigma-Aldrich, St. Louis, MO, USA. The companies from which the antibody, antigen solutions and modification agents were purchased are in the Supplementary Material. The device used for the fabricated immunosensor and the parameters of the electrochemical measurements were also given in Supplementary data.

### Procedures

#### Design of the CEST modified ITO-PET electrode

Before testing the biosensor's ability to determine TNF $\alpha$  concentration, the working electrode must be free of contaminants and cleaned. For cleaning procedure, the electrodes were given a ten-minute sonic bath in acetone, a soap solution, and ultra pure water.

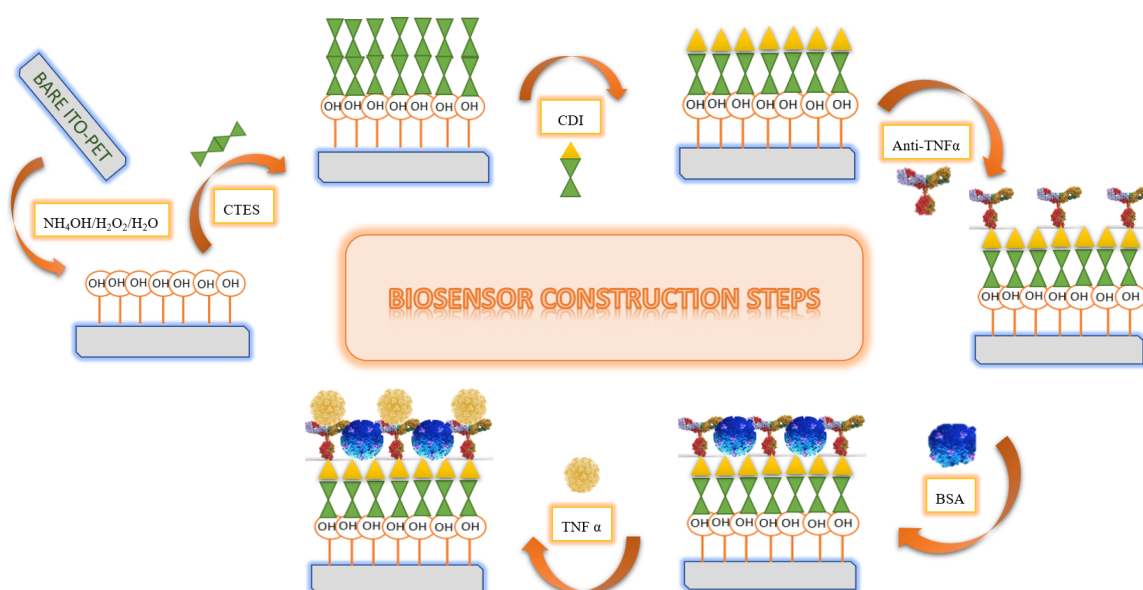
The sonication for 10 minutes was performed separately for these three solvents. Electrode surfaces were cleaned and then hydroxylated. As a result, Si-O-Si bonds on the surface were formed through the binding of the CEST silane agent. The hydroxylation process includes the incubation with ammonium hydroxide

(NH<sub>4</sub>OH)/ hydrogen peroxide (H<sub>2</sub>O<sub>2</sub>)/ ultra-pure water (1/1/5, v/v) solution for 90 minutes. The active ends of the CEST agent which allow the covalent binding of the antibody were carboxyl groups. The carbonyl diimidazole (CDI) solution was used to activate the carboxyl ends of the CEST solution. Afterwards, CEST modified electrode was incubated in anti-TNF $\alpha$  antibody. To prevent the nonspecific interactions and to block the unbound carboxyl groups, bovine serum albumin (BSA) blocking agent was used. Ultra-pure water was used to carefully rinse the electrode surfaces after each procedure. The biosensors were stored at +4 °C until being used in the TNF $\alpha$  analysis. The immobilization procedure and the modification steps are given in Scheme 1.

## RESULTS and DISCUSSION

### Immobilization procedure of the TNF $\alpha$ immunosensor

To regulate the physical and chemical properties of solid surfaces, self-assembling monolayers (SAM) are frequently employed. For electroanalytical purposes, SAM is frequently used in specific electrode design. Silaning agents are often preferred for the bioreagent immobilization to flexible ITO-PET electrodes. The immobilization processes can be listed step by step as follows: hydroxylation of the ITO-PET electrode surface, silanization of the hydroxylated electrode surface, activation of the carboxyl groups of the CEST solution, immobili-



**Scheme 1.** Immobilization scheme of the ITO-PET/OH/CEST/CDI/anti-TNF $\alpha$ /BSA/TNF $\alpha$  based biosensor.

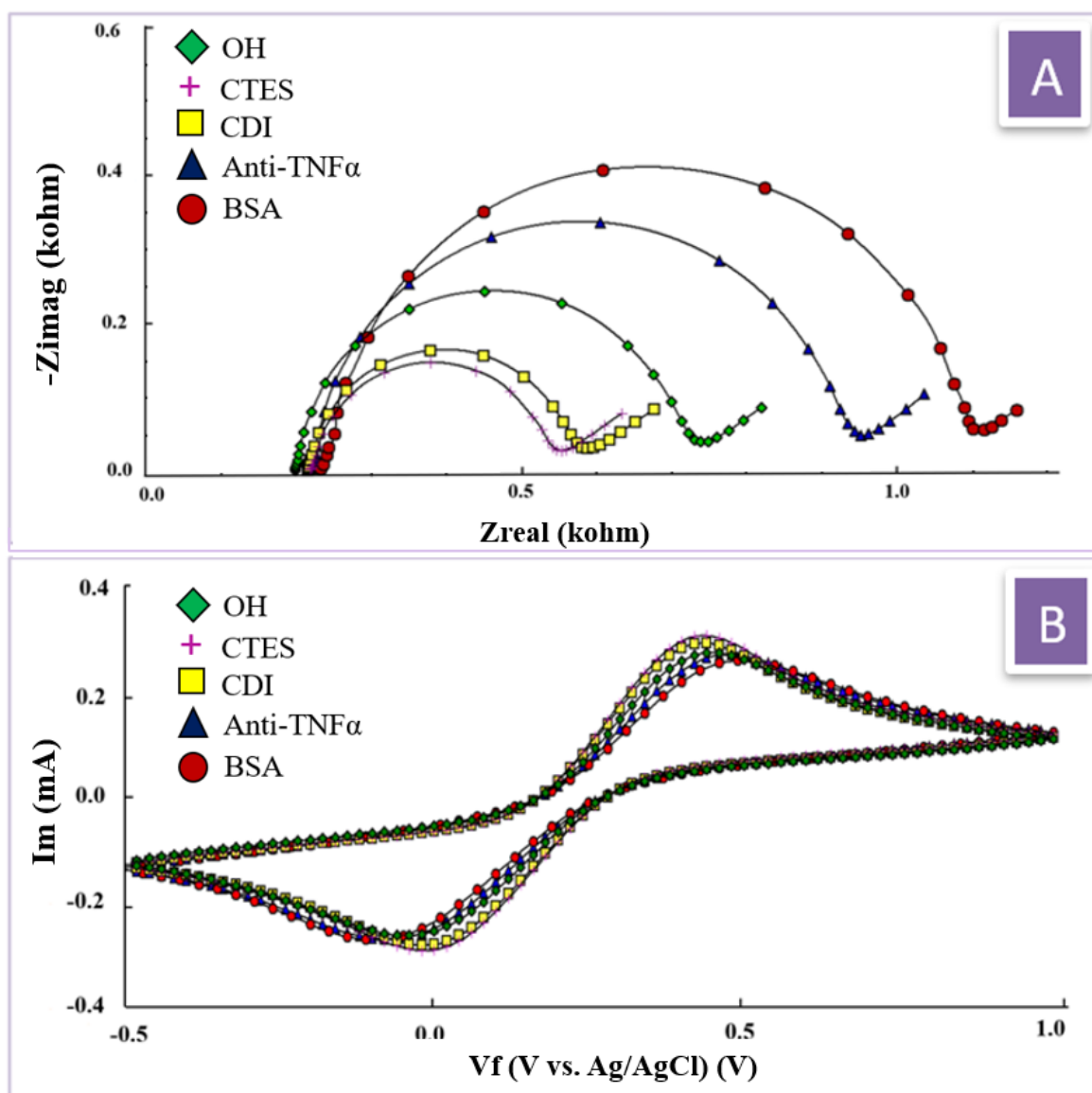


**Figure 1.** A) The impedance measurements and B) cyclic voltammograms belonging to the construction steps of the biosensor.

zation of the antibody to the surface, blocking of the surface with BSA solution, interactions between the antibody and antigen solutions.

To begin, the electrodes needed to be cleaned so that the final system would be clean and linear. The electrodes that were completely bare were subjected to sonication with acetone, soap solution, and ultra-pure water. Before the anti-TNF $\alpha$  antibody could be covalently immobilized onto the ITO-PET surface, the hydroxylated terminals needed to be treated with a silanization agent conjugated with indium tin oxide. The bare flexible electrodes were hydroxylated by being immersed in a solution of NH<sub>4</sub>OH: H<sub>2</sub>O<sub>2</sub>:H<sub>2</sub>O (1:1:5, v/v). After having

their surfaces hydroxylated, the electrodes were left overnight in a CEST solution. Silicones (RSi(OH)<sub>3</sub>) play a crucial role as intermediates in creating crosslinked silicones and as modification agents for biosensors [30]. After CEST modification, the antibody solution was covalently immobilized onto the surface via the interactions between carboxyl groups of the CEST agent and the amine groups of the anti-TNF $\alpha$  solution. In order to maximize the efficiency of the antibody-antigen interactions, the BSA solution was used to inactivate the unbounded carboxyl groups with the amine groups in the antibody solution. The immobilization procedures are depicted in Fig. 1A and 1B via EIS spectra and CV voltammograms, respectively.

By using  $\text{Fe}(\text{CN})_6^{3-/4-}$  as an indicator, electrochemical impedance spectroscopy (EIS) can be used to learn about the changes that occur at the electrode-electrolyte interface as a result of catalytic reactions, DNA hybridization or the interaction of the antigen-antibody. The EIS spectrum has two distinct components. The semi-circular zone at more elevated frequencies shows the charge transfer resistance, while the low-frequency Warburg impedance indicates the delay generated by the diffusion of electroactive species to the electrode [31]. Fig 1A presents the EIS spectra belonging to the hydroxylation of the surface, silanization process on the surface, activation of the carboxylated ITO-PET electrode surface, antibody immobilization, BSA blocking and interactions

between the antibody and the antigen solution. The first step and the green curve show the hydroxylation procedure. The ITO-PET electrode has a semi-conductive characteristic. The Nyquist diagram was too low when the -OH groups were formed on the surface. The semicircular diameter in the Nyquist diagram is also attributed to the resistance of the electron transfer ( $R_{ct}$ ) at the surface. The lower semicircular diameter in the Nyquist diagram demonstrates the higher conductivity of the surface. The formation of the hydroxyl groups provides a very conductive surface. Afterwards, the  $R_{ct}$  value was increased after the silanization with the CEST solution because of the negative carboxyl groups of the solution. The carboxyl groups of the CEST solution hin-

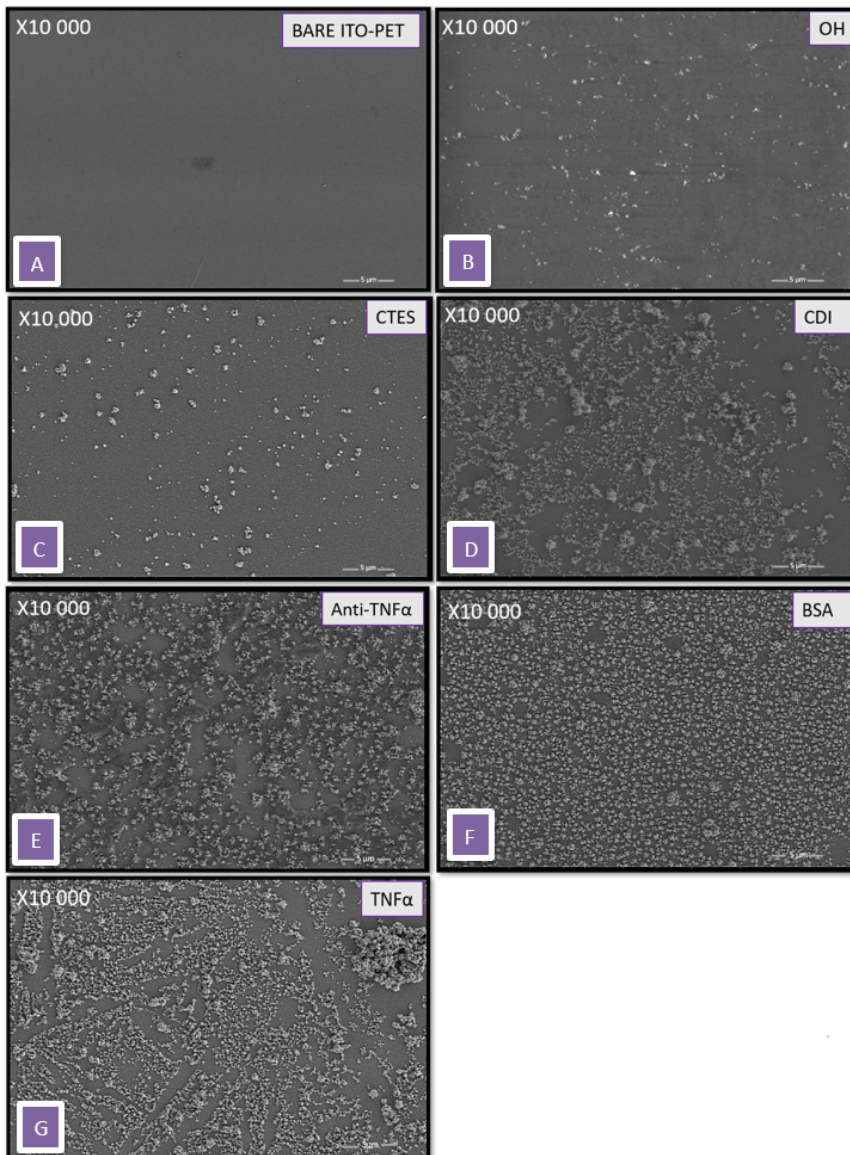


**Figure 2.** Morphological view of the modification procedures A) bare ITO-PET B) OH C) CEST D) CDI E) anti-TNF $\alpha$  F) BSA G) TNF $\alpha$ .

dered the diffusion of the ferri-ferro solution used as an electroactive redox probe to the surface. Anti-TNF $\alpha$  antibody was covalently immobilized onto the surface via the carboxyl groups of the CEST solution. Because of the barrier effect created by the antibody solution, electrons could not reach the surface. So, the semi-circular diameter in the Nyquist curve increased in EIS spectra. Afterwards, the BSA blocking stage increased the non-conductivity and the semicircular diameter of the Nyquist curve. The charge transfer resistance and the diffusion of the ferri-ferro redox probe were hindered with BSA treatment.

CV analysis was used to elaborate on the electrochemical activity of the ferri-ferro oxidation / reduction solution and surface differences throughout each immobilization protocol. The voltammetry technique is an effective method applied in electroanalytical chemistry and is frequently used in evaluating the effect of the environment on redox processes, elucidating reaction mechanisms, examining the stability of reaction products, obtaining modified surfaces, and illuminating the coating and complex structures with the use of various redox probes [32]. In cyclic voltammetry, the change in current versus potential values in a constantly changing range is plotted. Fig 1B presents the CV voltammograms belonging to the immobilization protocol of the TNF $\alpha$  immunosensor system. Since the transfer of the electron to the electrode surface could be provided very efficiently with the hydroxylation of the surface, the anodic and cathodic peak currents could be seen highly in the voltammograms. After the silanization process with **CEST** solution, the anodic and cathodic peak currents were decreased because of the difficulty in diffusing of the ferri-ferro redox probe to the hydroxylated surface. The negative carboxyl groups pushed the negatively charged ferri-ferro redox probe. After activation of the carboxyl groups on the electrode surface with CDI agent, the modified electrodes were immobilized with anti-TNF $\alpha$  solution. The peak currents were decreased because of the barrier effect of the antibody. The antibody solution increased the nonconductivity of the modified ITO-PET electrode surface. Finally, the anodic and cathodic peak currents again decreased due to the fact that the surface became more and more non-conductive.

#### Morphological imaging of the modified electrodes

The SEM technique allows for the step-by-step monitoring of morphological changes on the surface of the

biosensor. Fig. 2 displays Scanning Electron Microscopy (SEM) images for the immobilization stages of the immunosensor. The morphological view of the bare electrode surface is given in Fig. 2A. Because no modification process was applied to the surface, it appeared homogeneous. Fig 2B presents the hydroxylated surface morphologically. Afterwards, the electrode was incubated in CEST solution overnight. The surface belonging to the step of the CEST modification is given in the Fig 2C. Figure 2D shows the appearance after the carboxyl groups were activated by CDI solution. Fig 2E shows the anti-TNF $\alpha$  immobilization step. The surface showed a major morphological change, as shown in Fig 2E, and a dense layer emerged. Surface morphology changed during the BSA solution incubation phase, as shown in Fig. 2F. A denser, more spherical surface was achieved after treatment with BSA, as seen in Fig. 2F. A clustered and dense surface was observed, after the incubation of the electrode in TNF $\alpha$  solution and the interaction between anti-TNF $\alpha$  and TNF $\alpha$ . (Fig. 2G)

#### Determination of optimum parameters for the proposed biosensor

To create a linear and repeatable biosensor, all of the fundamental parameters including CEST concentration, CDI concentration, anti-TNF $\alpha$  concentration, CDI and the antibody incubation periods were optimized.

The concentration of CEST is a crucial factor in determining the surface stability and immobilization efficiency of the anti-TNF $\alpha$ . The electrode surfaces were hydroxylated, and then the solutions of varying concentrations of CEST (0.1%, 0.5%, and 1%) were applied to them. The EIS and CV measurements were used to examine the biosensor's sensitivity to TNF $\alpha$  concentrations. As the CEST concentrations increased (from 0.1% to 1%) the electrode surface may have degraded, leading to a lower charge transfer resistance. Therefore, the optimum CEST silanization agent concentration was chosen as 0.1% (Fig 3A).

After the incubation of the electrodes in CEST solution, the carboxyl groups of this agent were activated with CDI solution. CDI concentration, the other critical parameter that needed to be optimized, was investigated for designing a linear and effective immunosensor. For this purpose, four different concentrations of CDI solution (0.01 M, 0.05 M, 0.1 M, 0.25 M) were studied and calibration graphs for each concentration were obtained. The results demonstrated that the signals and the Rct

values were increased when the concentration of the CDI was increased from 0.01 M to 0.05 M. However, the interactions between the antibody and the antigen solution were weaker than the higher CDI concentrations from 0.05 M. Because the CDI concentration is also an important step for successful immobilization of the anti-TNF $\alpha$  solution. The higher CDI concentrations from 0.05 M (0.1 M and 0.25 M) showed negative effect on the antibody immobilization to the surface. Thus, the optimum CDI concentration was chosen as 0.05 M (Fig 3B).

The other studied parameter was optimum incubation time of the CDI solution. For this purpose, three different incubation periods (30 min, 45 min and 60 min) were investigated to obtain a linear and successful immunosensor system. When the CDI concentrations were increased, the biosensor signals and efficiency decreased. The increase in the incubation time of the CDI solution may result in irregular binding of the anti-TNF $\alpha$  solution. Accordingly, the optimal period for the incubation was chosen as 30 min (Fig 3C).

The concentration of the antibody is another variable that must be optimized for the best results. Four different concentrations of anti-TNF $\alpha$  solution (2 ng mL $^{-1}$ , 10 ng mL $^{-1}$ , and 50 ng mL $^{-1}$ ) were tested to determine the impact of anti-TNF $\alpha$  on the answer of the CEST-modified ITO-PET sensing platform. Using EIS data, calibration curves were drawn after subjecting biosensors manufactured with the different anti-TNF $\alpha$  concentrations to a range of TNF $\alpha$  antigen concentrations. When the antibody concentration was increased (from 2 ng mL $^{-1}$  to 10 ng mL $^{-1}$ ) the obtained signals were increased. This demonstrated that the low concentration of anti-TNF $\alpha$  (2 ng mL $^{-1}$ ) was inadequate to interact with the TNF $\alpha$  solution. However, the impedimetric biosensor was found to be less sensitive at higher concentration levels of the antibody (50 ng mL $^{-1}$ ). A more complex bioactive layer was likely formed after incubating the electrodes with anti-TNF $\alpha$  at higher concentrations, which resulted in nonselective binding to the surface. Due to these factors, 10 ng mL $^{-1}$  of anti-TNF $\alpha$  concentration was chosen as the most effective and optimum concentration. (Fig 3D).

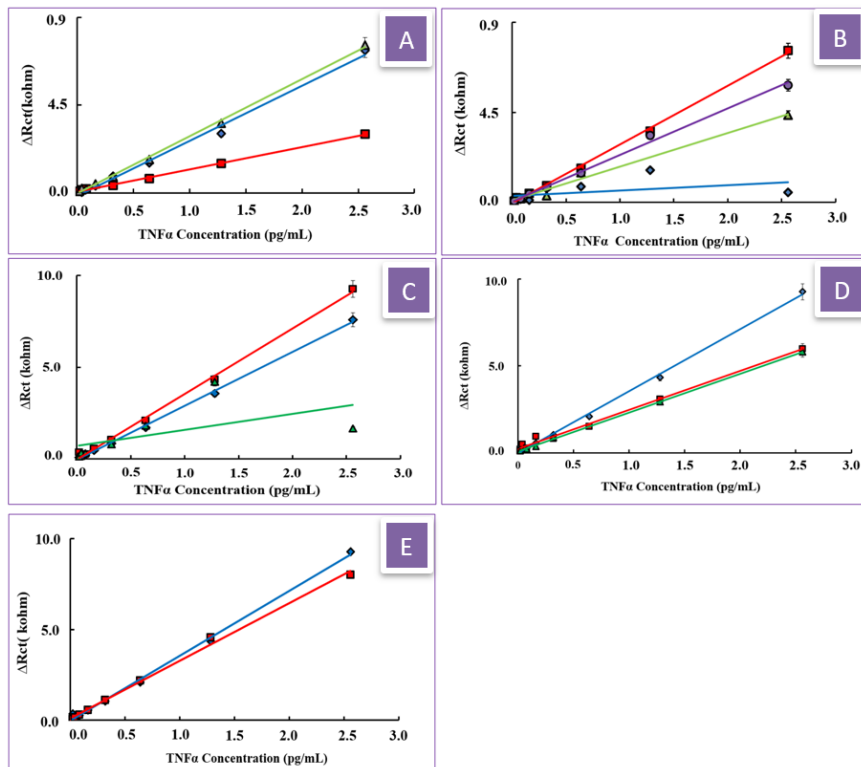


**Figure 3.** A) The effect of the CEST concentration on the immunosensor response ( $\blacktriangle$ : 0.1% CEST,  $\blacklozenge$ : 0.5% CEST,  $\blacksquare$ : 1% CEST) B) The effect of the CDI concentration on the immunosensor response ( $\blacklozenge$ : 0.01 M CDI,  $\blacksquare$ : 0.05 M CDI,  $\blacklozenge$ : 0.1 M CDI,  $\blacktriangle$ : 0.25 M CDI) C) The effect of the CDI incubation time on the immunosensor response ( $\blacksquare$ : 30 min CDI,  $\blacklozenge$ : 45 min CDI,  $\blacktriangle$ : 60 min CDI) D) The effect of the anti-TNF $\alpha$  concentration on the immunosensor response ( $\blacktriangle$ : 2 ng mL $^{-1}$  anti-TNF $\alpha$ ,  $\blacklozenge$ : 10 ng mL $^{-1}$  anti-TNF $\alpha$ ,  $\blacksquare$ : 50 ng mL $^{-1}$  anti-TNF $\alpha$ ) E) The effect of the anti-TNF $\alpha$  incubation time on the immunosensor response ( $\blacklozenge$ : 30 min anti-TNF $\alpha$ ,  $\blacksquare$ : 45 min anti-TNF $\alpha$ ).

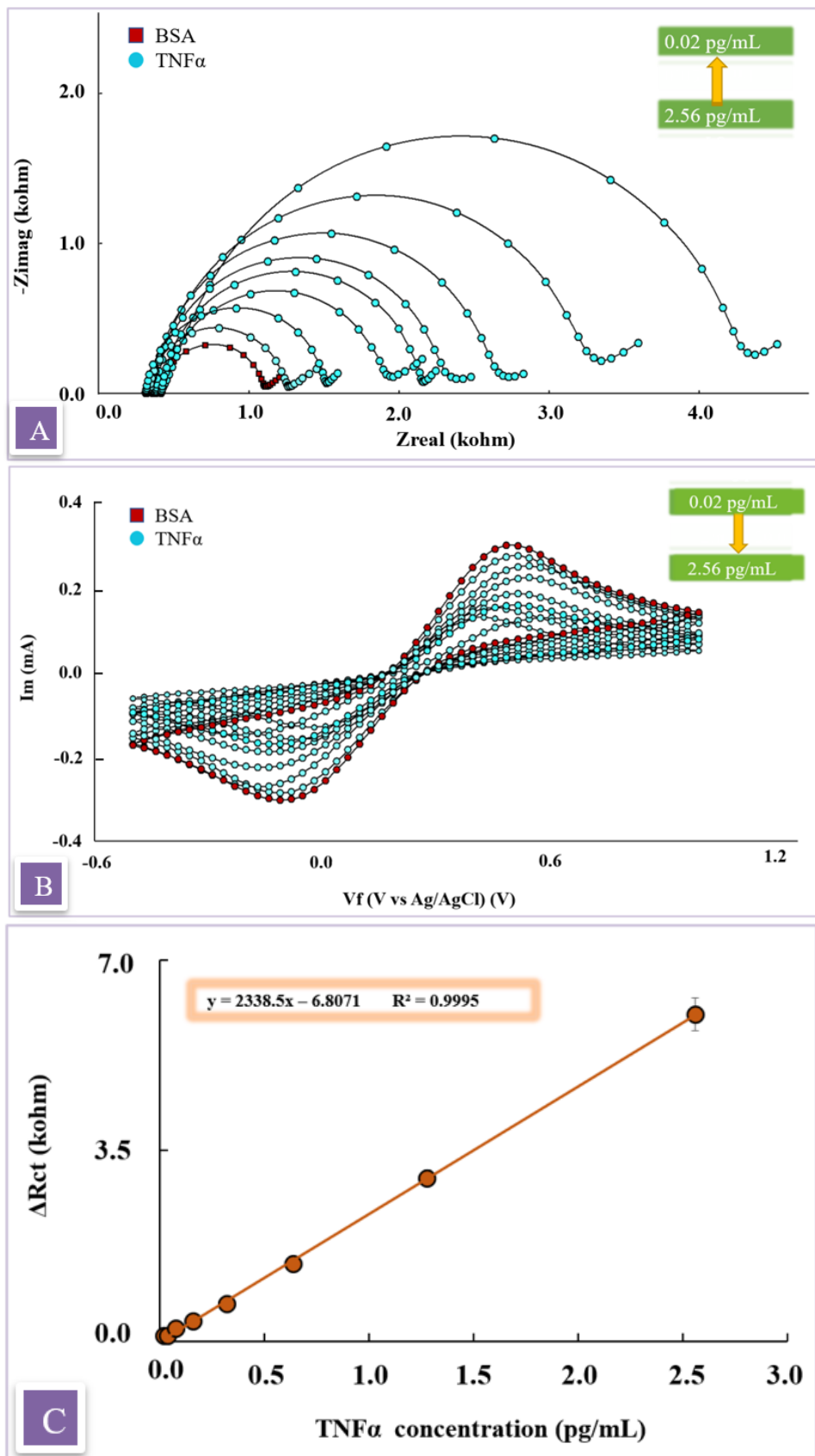


**Figure 4.** A) Impedance measurements B) Cyclic voltammograms belonging to the increasing TNF $\alpha$  concentrations C) Calibration graph of the TNF $\alpha$  biosensor.

Following the step which consisted of determining the optimal antibody concentration, the next step involved determining the optimal antibody incubation time. Anti-TNF $\alpha$  antibody was used to incubate CEST-modified ITO-PET electrodes for two different durations (30 min and 45 min). Due to the proximity of the 30-min and 45-min signals and great  $R^2$  values for the two periods of antibody incubation, the optimum time was chosen as 30 min. Increasing the incubation time of the anti-TNF $\alpha$  did not significantly increase the efficiency of the biosensor and the antibody-antigen interactions (Fig 3E).

### Characterization analyses of the TNF $\alpha$ biosensor design

When the immobilization process was perfected, the linear detection range of the TNF $\alpha$  immunosensor was examined. The optimally prepared ITO-PET electrodes were then applied to TNF $\alpha$  solutions of increasing concentrations. The following equation was used to create the linear graph of the TNF $\alpha$  immunosensor. The Rct values were obtained from EIS measurements.

$$\Delta Rct = Rct_{(TNF\alpha)} - Rct_{(BSA)}$$

The value of Rct after anti-TNF $\alpha$ -TNF $\alpha$  binding is denoted by  $Rct_{(TNF)}$ . After blocking the anti-TNF $\alpha$  immunosensor with BSA, the value of Rct is denoted by  $Rct_{(BSA)}$ . Figures 4A and 4B depict the Nyquist plots and the electrochemical voltammograms of CV measurements of the TNF $\alpha$  immunosensing system. While incubating the electrodes in increasing TNF $\alpha$  antigen concentrations led to higher Rct values in EIS measurements, it resulted in lower cathodic and anodic peak currents in CV voltammograms. As TNF $\alpha$  solution concentrations

increased, electrode surfaces became more insulative, causing electron transfer more difficult. A determination range of 0.02 pg mL $^{-1}$  to 2.56 pg mL $^{-1}$  was demonstrated by the calibration curve (Fig. 4C), which had a determination coefficient ( $R^2$ ) of 0.9995. The great wide and low concentration range demonstrated the ultra-high sensitivity of the constructed ITO-PET immunosensor.

One of the most crucial aspects of characterizing a biosensor is studying its repeatability. As a result, twenty different constructed electrodes, all of which were applied to the same TNF $\alpha$  concentrations (1.5 pg mL $^{-1}$ ), were compared. Coefficient of variation (3.76 %), standard deviation (0.056647 pg mL $^{-1}$ ), and mean value (1.503 pg mL $^{-1}$ ) were all calculated to demonstrate the high degree of repeatability of the immunosensor.

Six different immunosensors were prepared using the same method for analyzing TNF $\alpha$  concentrations ranging from 0.02 pg mL $^{-1}$  to 2.56 pg mL $^{-1}$ , and their results were compared to determine the reproducibility of the developed biosensor (Fig 5). The calibration graphs of six different biosensors were plotted via the EIS spectra given in Fig. 4A. These ITO-PET-based biosensors exhibited comparable performance for TNF $\alpha$  concentrations ranging from 0.02 pg mL $^{-1}$  to 2.56 pg mL $^{-1}$ . With the help of the linear equations presented in Fig. 5, the RSD % value for the slope data was determined to be 2.08 %. Studies of reproducibility that corroborate the high sensitivity and reliability of the biosensor proved that the TNF $\alpha$  immunosensor design was successful and remarkable.

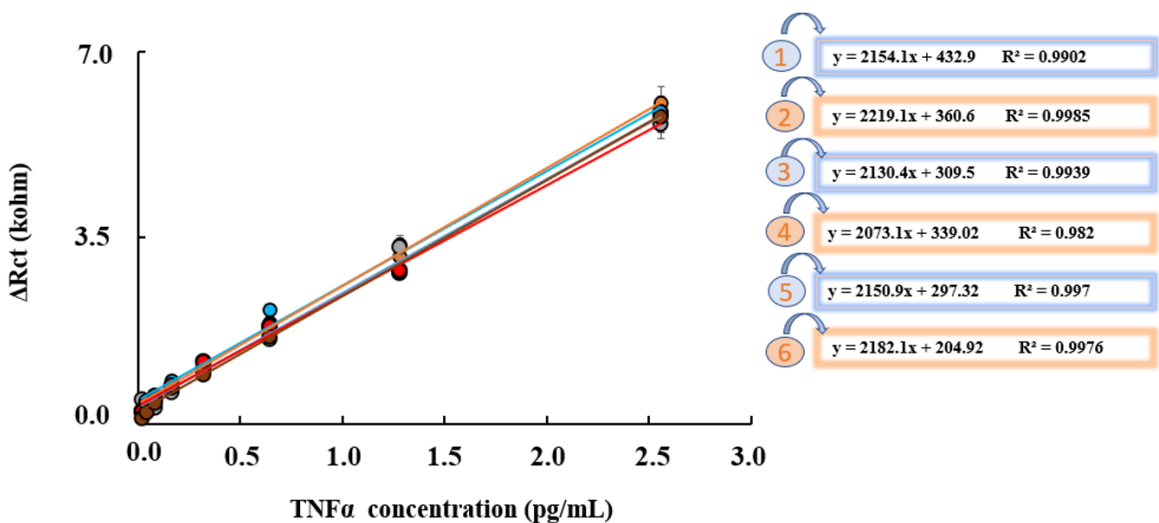


Figure 5. Reproducibility study.

Repeated use of a biosensor at a constant analyte concentration over time results in a stable and robust signal, a property known as stability. The storage stability of the built ITO-PET-based disposable immunosensor was assessed by evaluating the immunosensor response with weekly EIS measurements (Fig 6A). It was observed that the system preserved 94.17% of its stability for 9 weeks, and a significant activity loss in the impedance signal appeared after the ninth week. After ten weeks, the biosensor retained 46.42 % of its activity, as recorded. This demonstrates that the fabricated biosensor system has an efficient capacity for storage.

TNF $\alpha$  biosensor regeneration capacity was ensured by treating the ITO-PET electrode built under ideal conditions with TNF $\alpha$  solution and then treating it with 0.1% HCl solution. Bioelectrodes were immersed in an acidic solution for 5 minutes after being used to measure TNF $\alpha$  antigen. The signals collected during EIS measurements were analyzed. In the acid treatment step, the semicircle diameter of the Nyquist curve decreased compared to the TNF $\alpha$  incubation step. Because anti-TNF $\alpha$  and TNF $\alpha$  solution rely on weak interactions, such

as Van der Waals or hydrogen bonding, and an acid solution can destroy these bonds. The process was repeated until no usable signal could be interpreted from the bioelectrode. In the first regeneration step, almost all of the biosensor activity was preserved. After the fifth regeneration, 98.16% of the activity was preserved. After the eighth regeneration, 96.9% of the electrode's original activity remained. Afterwards, significant activity losses were observed and the life of the biosensor came to an end. In the ninth regeneration, the electrode lost 22.6% of its activity. In the eleventh step, the electrode lost almost all of its usability capacity (Fig 6B).

The Kramers-Kronig transformation was utilized to evaluate whether external variables affected the impedance spectrum of the created TNF $\alpha$  biosensor system. The experimental data and the estimated Kramers-Kronig transformations cannot overlap in this strategy if the biosensor is impacted by variances from external influences [33]. Fig. 6C demonstrates that the accuracy and stability of the biosensor are confirmed by the overlap between Kramers Kronig transforms and experimental data.

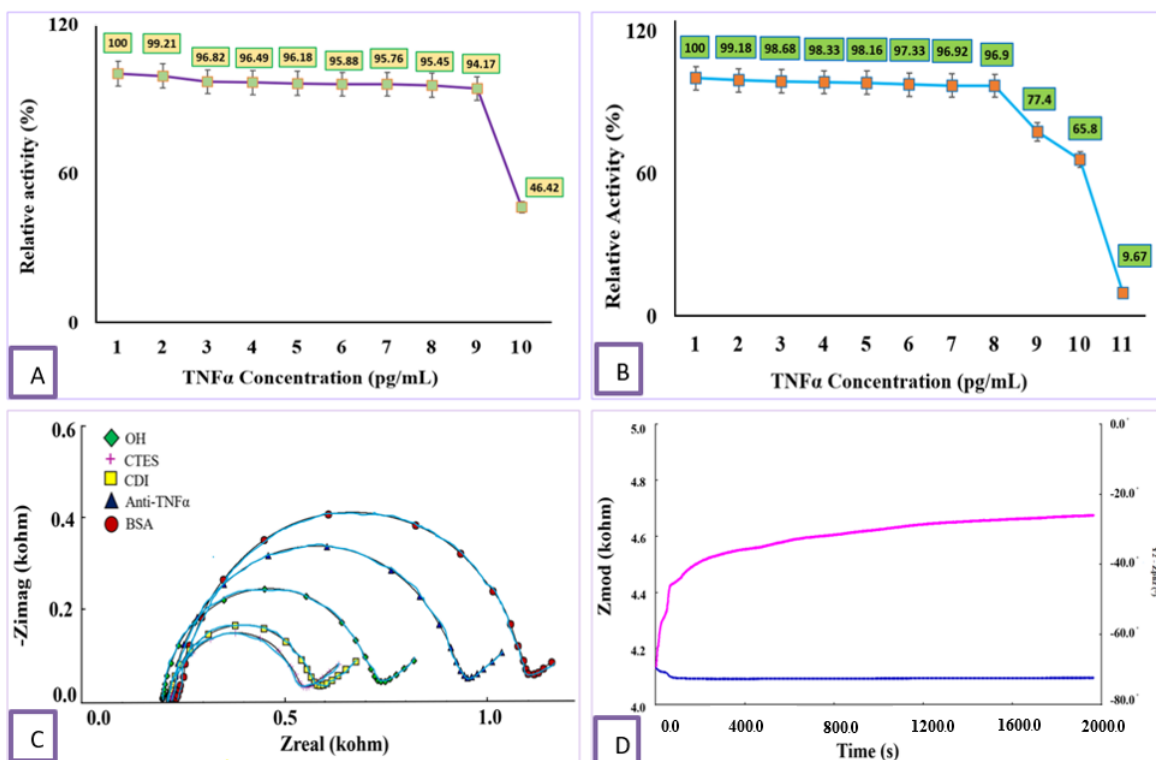


**Figure 6.** A) Storage capacity of the biosensor B) Regeneration study of the biosensor C) Kramers Kronig transform D) The impedance measurement at a single frequency (pink curve: change in impedance, blue curve: change in phase angle).

**Table 1.** Analyzing TNF $\alpha$  in actual human serum using the suggested immunosensor.

Serum	Determined by biosensor (pg mL <sup>-1</sup> )	Added TNF $\alpha$ concentration (pg mL <sup>-1</sup> )	Total found by biosensor (pg mL <sup>-1</sup> )	RSD (%) (n=3)	Recovery (%)
1	2.11	0.16	2.27/ 2.28/ 2.28	0.44	100.44
		0.32	2.42/ 2.44/ 2.41	0.41	99.59
2	1.42	0.16	1.57/ 1.58/ 1.50	1.89	98.11
		0.32	1.75/ 1.76/ 1.78	1.15	101.15
3	0.54	0.16	0.66/ 0.67/ 0.74	1.43	98.57
		0.32	0.89/ 0.89/ 0.79	0.35	99.65
4	1.26	0.16	1.42/ 1.44/ 1.45	1.4	101.4
		0.32	1.53/ 1.58/ 1.61	0.63	99.37
5	1.01	0.16	1.22/ 1.14/ 1.18	0.85	100.85
		0.32	1.30/ 1.46/ 1.27	0.75	100.75

**Table 2.** Research of the literature to contrast the proposed biosensor for TNF detection with previous studies.

Electrode	Immobilization method	Measurement method	Linear range	Reference
Nanofibers modified gold electrode	Polystyrene (PS)-polyamidoamine (PAMAM) dendritic polymer nanofibers	EIS	10–200 pg mL <sup>-1</sup>	[37]
SPE	Fullerene@MWCNTs (C60)-f-MWCNTs and ionic liquid 1-butyl-3-methylimidazolium bis (trifluoromethyl sulfonyl) imide	DPV	5pg mL <sup>-1</sup> -75 pg mL <sup>-1</sup>	[38]
ISFET	Ion Sensitive Field Effect Transistor (ISFET) based on silicon nitride	EIS	1pg mL <sup>-1</sup> -50 pg mL <sup>-1</sup>	[39]
Gold electrode	4-carboxymethylaniline modification	Chronoamperometric	1 pg mL <sup>-1</sup> - 30 pg mL <sup>-1</sup>	[40]
ITO-PET electrode	CEST modification	EIS and CV	0.02 pg mL <sup>-1</sup> - 2.56 pg mL <sup>-1</sup>	This study

### A Single Frequency Impedance Analysis of a TNF $\alpha$ Biosensor

An EIS methodology known as single-frequency-impedance (SFI) analysis reduces the complexness of a single frequency, signal processing, making it a practical, straightforward, and low-cost method [34]. Single frequency impedance technique (SFI) is an effective method for measuring impedance against time at a given frequency. This method was used to the immunosensor to investigate the interaction between TNF $\alpha$  antigen and anti-TNF $\alpha$  antibodies immobilized on a CEST-modified ITO-PET surface. Figure 6D depicts the SFI result of this biosensing technology. Biocomplex formation of anti-TNF $\alpha$  / TNF $\alpha$  was observed using impedance measurements in a pH 7.0 phosphate buffer at a constant frequency of 45 Hz for 2000 seconds. It was determined that the electrode surface was saturated with TNF $\alpha$  protein after 2000 seconds when the impedance was nearly constant.

### Constructed ITO-PET based immunosensor for measuring TNF $\alpha$ in human serum

The created biosensor was evaluated by measuring TNF $\alpha$  in five separate serum samples to see whether it was clinically applicable. The ethical committee of Tekirdağ Namık Kemal University, with the approval number 2013/86/07/05, allowed the collection of serum samples from Tekirdağ Namık Kemal University Faculty of Medicine. The standard addition technique to human serum was used to evaluate the analytical accuracy of the manufactured immunosensor. According to studies of healthy males and females, TNF $\alpha$  levels in human serum are typically lower than 40 pg mL<sup>-1</sup> for healthy humans [35]. The level of this antigen was found in the articles that studied different control groups of healthy individuals. According to Li and co-workers, serum levels of TNF $\alpha$  are 9.20 (7.70–10.60) pg mL<sup>-1</sup> [36]. The obtained data from these references are detectable by our biosensor system after the required dilution. All serum samples were diluted 10-fold. Since the concentration of TNF $\alpha$  in serum from healthy individuals was higher than the detection range of the built biosensor, real serum samples were diluted to the required concentrations. Table 1 displays the recovery results and the RSD% values obtained with the fabricated immunosensor system employing the standard addition method. Having the ability to use biosensors in the medical field could have huge commercial and precision benefits. Based on the findings, it appears that the developed biosensor can detect TNF $\alpha$  in human serum samples and could be adapted for use in clinical environments.

The analytical efficiency of the produced immunosensor was compared with that of other sensor systems built for TNF determination in Table 2. Razmshoar and co-workers [37] developed polystyrene (PS)-polyamidoamine (PAMAM) dendritic polymer nanofibers based biosensor system. The obtained biosensor by Razmshoar could detect the TNF $\alpha$  concentrations between 10–200 pg mL<sup>-1</sup>. Ardakani and co-workers [38] fabricated SPE based biosensor for TNF $\alpha$  detection. The linear range of the biosensor was obtained as 5pg mL<sup>-1</sup>–75 pg mL<sup>-1</sup>. When the studies given in Table 2 were investigated, the sensitivity of the biosensors were lower than the proposed CEST-modified biosensor system. The ITO-PET based immunosensor showed great wide detection range compared to the other studies. The data seen in the Table 2 demonstrate that the designed ITO-PET based immunosensor system has a lot of great features such as high sensitivity, low detection limit or great wide detection range. Also, the proposed biosensor presents a very practical method. The construction steps of the biosensor are very easy-prepared.

**Acknowledgments** - The Scientific and Technological Research Council of Turkey, TÜBİTAK, provided funding for this investigation. This help is greatly appreciated (Project ID: 113 Z 678).

---

### References

1. S.M.I. Bari, L.G. Reis, G.G. Nestorova, Calorimetric sandwich-type immunosensor for quantification of TNF- $\alpha$ , *Biosens. Bioelectron.*, 126 (2019) 82–87.
2. H. Filik, A.A. Avan, Electrochemical immunosensors for the detection of cytokine tumor necrosis factor alpha: a review, *Talanta*, 211 (2020) 120758.
3. X. Mei, J. Wang, C. Zhang, J. Zhu, B. Liu, Q. Xie, T. Yuhan, Y. Wu, R. Chen, X. Xie, Y. Wei, L. Wang, G. Shao, Q. Xiong, Y. Xu, Z. Feng, Z. Zhang, Apigenin suppresses mycoplasma-induced alveolar macrophages necroptosis via enhancing the methylation of TNF- $\alpha$  promoter by PPAR $\gamma$ -Uhrf1 axis, *Phytomedicine*, 108 (2023) 154504.
4. I.A. Bhat, I.R. Mir, G.H. Malik, J.I. Mir, T.A. Dar, S. Nisar, N.A. Naik, Z. Sabah, Z.A. Shah, Comparative study of TNF- $\alpha$  and vitamin D reveals a significant role of TNF- $\alpha$  in NSCLC in an ethnically conserved vitamin D deficient population, *Cytokine*, 160 (2022) 156039.
5. X. Fan, X. Xu, X. Wu, R. Xia, F. Gao, Q. Zhang, W. Sun, The protective effect of DNA aptamer on osteonecrosis of the femoral head by alleviating TNF- $\alpha$ -mediated necroptosis via RIP1/RIP3/MLKL pathway, *J. Orthop. Translat.*, 36 (2022) 44–51.
6. M.D.C. Surboyo, R.M. Boedi, N. Hariyani, A.B.R. Santosh, I.B.P.P. Manuaba, P.H. Cecilia, I.G.A.D. Ambarawati, A.E. Parmadiati, D.S. Ernawati, The expression of TNF- $\alpha$  in recurrent aphthous stomatitis: A systematic review and meta-analysis, *Cytokine*, 157 (2022) 155946.

7. C.W. Hu, Y.C. Chang, C.H. Liu, Y.A. Yu, K.Y. Mou, Development of a TNF- $\alpha$ -mediated Trojan Horse for bacteria-based cancer therapy, *Mol. Ther.*, 30 (2022) 2522-2536.
8. A. Ghods, F. Mehdipour, R. Rasolmali, A.R. Talei, A. Ghaderi, The expression pattern of membranous TNF- $\alpha$  is distinct from its intracellular form in breast cancer-draining lymph nodes, *Clin. Immunol.*, 238 (2022) 109026.
9. A.J. Freeman, C.J. Kearney, J. Silke, J. Oliaro, Unleashing TNF cytotoxicity to enhance cancer immunotherapy, *Trends Immunol.*, 42 (2021) 1128-1142.
10. A.G. Alotaibi, J.V. Li, N.J. Gooderham, Tumour necrosis factor- $\alpha$  (TNF- $\alpha$ ) enhances dietary carcinogen-induced DNA damage in colorectal cancer epithelial cells through activation of JNK signaling pathway, *Toxicology*, 457 (2021) 152806.
11. H. Kitaura, A. Marahleh, F. Otori, T. Noguchi, Y. Nara, A. Pramusita, K. Ma, K. Kanou, I. Mizoguchi, Role of the interaction of tumor necrosis factor- $\alpha$  and tumor necrosis factor receptors 1 and 2 in bone-related cells, *Int. J. Mol. Sci.*, 23 (2022) 1481.
12. M. Liu, Y. Li, X. Liu, Serum tumor necrosis factor- $\alpha$ , interleukin-1 $\beta$ , interleukin-6, and interleukin-17 relate to anxiety and depression risks to some extent in non-small cell lung cancer survivor, *Clin Respir J.*, 16 (2022) 105-115.
13. D. Cruceriu, O. Baldasici, O. Balacescu, I. Berindan-Neagoe, The dual role of tumor necrosis factor-alpha (TNF- $\alpha$ ) in breast cancer: molecular insights and therapeutic approaches, *Cell. Oncol.*, 43 (2020) 1-18.
14. A.A. Abdellatif, M. Alsharidah, O. Al Rugaie, H.M. Tawfeek, N.S. Tolba, Silver nanoparticle-coated ethyl cellulose inhibits tumor necrosis factor- $\alpha$  of breast cancer cells, *Drug Des. Devel. Ther.*, 15 (2021) 2035-2046.
15. B. Özcan, M.K. Sezginürk, Fabrication of an ultrasensitive and single-use graphite paper based immunosensor for Neuropeptide Y detection: A promising biosensing system for early detection of childhood obesity, *Mater. Today Commun.*, 33 (2022) 104797.
16. B. Demirbakan, M.K. Sezginürk, An electrochemical immunosensor based on graphite paper electrodes for the sensitive detection of creatine kinase in actual samples, *J. Electroanal. Chem.*, 921 (2022) 116656.
17. A. Azzouz, L. Hejji, K.H. Kim, D. Kukkar, B. Souhail, N. Bhardwaj, R.J.C. Brown, W. Zhang, Advances in surface plasmon resonance-based biosensor technologies for cancer biomarker detection, *Biosens. Bioelectron.*, 197 (2022) 113767.
18. C. Ozyurt, I. Uludağ, B. Ince, M.K. Sezginürk, Biosensing strategies for diagnosis of prostate specific antigen, *J. Pharm. Biomed. Anal.*, 209 (2021) 114535.
19. I.M. Mostafa, Y. Tian, S. Anjum, S. Hanif, M. Hosseini, B. Lou, G. Xu, Comprehensive review on the electrochemical biosensors of different breast cancer biomarkers, *Sens. Actuators B Chem.*, 365 (2022) 131944.
20. A. Mohammadpour-Haratbar, Y. Zare, K.Y. Rhee, Electrochemical biosensors based on polymer nanocomposites for detecting breast cancer: Recent progress and future prospects, *Adv. Colloid Interface Sci.*, 309 (2022) 102795.
21. Y. Li, R. Han, X. Yu, M. Chen, Q. Chao, X. Luo, An antifouling and antibacterial electrochemical biosensor for detecting aminopeptidase N cancer biomarker in human urine, *Sens. Actuators B Chem.*, 373 (2022) 132723.
22. A. Khodadoust, N. Nasirizadeh, S.M. Seyfati, R.A. Taheri, M. Ghanei, H. Bagheri, High-performance strategy for the construction of electrochemical biosensor for simultaneous detection of miRNA-141 and miRNA-21 as lung cancer biomarkers, *Talanta*, 252 (2023) 123863.
23. M. Çalışkan, B. Vural, M.K. Sezginürk, A Novel Disposable Immunosensor for Early Diagnosis of Cardiovascular Diseases, *ChemistrySelect*, 7 (2022) e202200061.
24. Y. Wang, B. Sun, H. Wei, Y. Li, F. Hu, X. Du, J. Chen, Investigating immunosensor for determination of depression marker-Apo-A4 based on patterning AuNPs and N-Gr nanomaterials onto ITO-PET flexible electrodes with amplifying signal, *Anal. Chim. Acta.*, 1224 (2022) 340217.
25. I. Uludağ, M.K. Sezginürk, Ultrasensitive and Cost-Effective Detection of Neuropeptide-Y by a Disposable Immunosensor: A New Functionalization Route for Indium-Tin Oxide Surface, *Biosensors*, 12 (2022) 925.
26. L. Kinner, M. Bauch, R.A. Wibowo, G. Ligorio, E.J. List-Kratochvil, T. Dimopoulos, Polymer interlayers on flexible PET substrates enabling ultra-high performance, ITO-free dielectric/metal/dielectric transparent electrode, *Mater. Des.*, 168 (2019) 107663.
27. M. Mousavi, E. Fini, Silanization mechanism of silica nanoparticles in bitumen using 3-Aminopropyl triethoxysilane (APTES) and 3-glycidyloxypropyl trimethoxysilane (GPTMS), *ACS Sustain. Chem. Eng.*, 8 (2020) 3231-3240.
28. W. Ran, H. Zhu, X. Shen, Y. Zhang, Rheological properties of asphalt mortar with silane coupling agent modified oil sludge pyrolysis residue, *Constr Build Mater.*, 329 (2022) 127057.
29. A. Villalonga, I. Estabiel, A.M. Pérez-Calabuig, B. Mayol, C. Parrado, R. Villalonga, Amperometric aptasensor with sandwich-type architecture for troponin I based on carboxyethylsilanetriol-modified graphene oxide coated electrodes, *Biosens. Bioelectron.*, 183 (2021) 113203.
30. T. Aziz, A. Ullah, H. Fan, M.I. Jamil, F.U. Khan, R. Ullah, M. Iqbal, A. Ali, B. Ullah, Recent progress in silane coupling agent with its emerging applications, *J Polym. Environ.*, 29 (2021) 3427-3443.
31. N.O. Laschuk, E.B. Easton, O.V. Zenkina, Reducing the resistance for the use of electrochemical impedance spectroscopy analysis in materials chemistry, *RSC Adv.*, 11 (2021) 27925-27936.
32. H.W. Wang, C. Bringans, A.J. Hickey, J.A. Windsor, P.A. Kilmartin, A.R. Phillips, Cyclic Voltammetry in Biological Samples: A Systematic Review of Methods and Techniques Applicable to Clinical Settings, *Signals*, 2 (2021) 138-158.
33. D.M. Solís, N. Engheta, Functional analysis of the polarization response in linear time-varying media: A generalization of the Kramers-Kronig relations, *Phys. Rev. B.*, 103 (2021) 144303.
34. N. Togasaki, T. Yokoshima, Y. Oguma, T. Osaka, Detection of Unbalanced Voltage Cells in Series-connected Lithium-ion Batteries Using Single-frequency Electrochemical Impedance Spectroscopy, *J. Electrochem. Sci. Technol.*, 12 (2021) 415-423.
35. S. Gao, Y. Cheng, S. Zhang, X. Zheng, J. Wu, A bilayer interferometry-based, aptamer-antibody receptor pair biosensor for real-time, sensitive, and specific detection of the disease biomarker TNF- $\alpha$ , *Chem. Eng. J.*, 433 (2022) 133268.

36. G. Li, W. Wu, X. Zhang, Y. Huang, Y. Wen, X. Li, R. Gao, Serum levels of tumor necrosis factor alpha in patients with IgA nephropathy are closely associated with disease severity, *BMC Nephrol.*, 19 (2018) 1-9.
37. P. Razmshoar, S.H. Bahrani, M. Rabiee, M. Hangouet, M. Martin, A. Errachid, N. Jaffrezic-Renault, A novel electrochemical immunosensor for ultrasensitive detection of tumor necrosis factor  $\alpha$  based on polystyrene-PAMAM dendritic polymer blend nanofibers, *Microchem. J.*, 175 (2022) 107206.
38. M.M. Ardakani, L. Hosseinzadeh, A. Khoshroo, Label-free electrochemical immunosensor for detection of tumor necrosis factor  $\alpha$  based on fullerene-functionalized carbon nanotubes/ionic liquid, *J. Electroanal. Chem.*, 757 (2015) 58-64.
39. H.B. Halima, F.G. Bellagambi, A. Alcacer, N. Pfeiffer, A. Heuberger, M. Hangouët, N. Zine, J. Bausells, A. Elaissari, A. Errachid, A silicon nitride ISFET based immunosensor for tumor necrosis factor-alpha detection in saliva. A promising tool for heart failure monitoring, *Anal. Chim. Acta.*, 1161 (2021) 338468.
40. L. Barhoumi, A. Baraket, F.G. Bellagambi, G.S. Karanasiou, M.B. Ali, D.I. Fotiadis, J. Bausells, N. Zine, M. Sigaud, A. Errachid, A novel chronoamperometric immunosensor for rapid detection of TNF- $\alpha$  in human saliva, *Sens. Actuators B Chem.*, 266 (2018) 477-484.